Tungsten (2020) 2:240–250
https://doi.org/10.1007/s42864-020-00055-5

Tungsten
www.springer.com/42864

REVIEW PAPER

Enhanced photocatalytic performance of tungsten-based photocatalysts for degradation of volatile organic compounds: a review

Qiang Cheng[1] · Gao-Ke Zhang[1]

Received: 13 May 2020 / Revised: 14 June 2020 / Accepted: 15 June 2020 / Published online: 1 September 2020

Abstract
Photocatalytic oxidation process for the degradation of volatile organic compounds (VOCs) contaminants is a promising technology. But until now, the low photocatalytic activity of the conventional TiO_2 photocatalyst under visible-light irradiation hinders the deployment of this technique for VOCs degradation. WO_3 has been proved to be a suitable photocatalytic material for degradation of various VOCs as its appropriate band-gap, high stability and great capability. Nevertheless, the actual implementation of WO_3 is still restricted by short lifetime of photoexcited charge carriers and low light energy conversion efficiency: its photocatalytic performance is needed to be improved. This review discusses the process of tungsten-based photocatalyst for removal of VOCs and summarizes a variety of strategies to improve the VOCs oxidation performances of WO_3, such as controlling the morphology structure, engendering chemical defects, coupling heterojunction, doping suitable dopants and loading a co-catalyst. In addition, the practical application of tungsten-based photocatalyst is discussed.

Keywords Tungsten trioxide · Photocatalytic oxidation · Volatile organic compound degradation · Modification

1 Introduction

Volatile organic compounds (VOCs), which mainly contain alkanes, aromatics, alkenes, carboxylic acids, esters and alcohols [1], have been proven to seriously damaged environment and human health owning to their toxic carcinogenesis and environmental destructiveness such as photochemical smog, greenhouse effect and stratospheric ozone depletion. To solve this problem, several effective VOC elimination techniques such as adsorption [2], ozonation [3], chemical combustion [4], biological degradation [5] and photocatalytic oxidation [6–8] have been proposed in recent decades. Among the above methods, photocatalytic oxidation technology is a promising method for removing gaseous pollutants with a low concentration, owing to its excellent features of operation at room temperature and high activity towards various pollutants which can react to final products (CO_2 and H_2O) [9–11]. This technology is basically founded on the application of semiconductor materials with ultraviolet (UV) light at ambient temperature [12, 13]. For instance, TiO_2 is regarded as the appropriate semiconductor photocatalyst for converting various VOCs into less harmful molecules due to its low cost, high stability and great capability [14].

Despite its advantages for VOC degradation, some challenges with TiO_2 cannot be ignored. For instance, intrinsic large band-gap limited its application to high wavelength region under visible light. In addition, high recombination rate of photo-generated charge carriers, which lowers the photocatalytic application on photocatalysis oxidation under visible light or natural solar light irradiation. Furthermore, the photocatalytic oxidation efficiency is reduced by the high recombination of electrons (e^-) and holes (h^+). Therefore, photocatalysis process should gain considerable attention to seek highly efficient photocatalysts, which can slow down the recombination rate, accelerate the charge separation efficiency and also respond to visible light absorption [15, 16].

Compared with TiO_2 and other semiconductor materials, WO_3 has become the ideal choice for photocatalytic oxidation of VOCs due to its exhibition of broader wavelength

✉ Gao-Ke Zhang
gkzhang@whut.edu.cn

[1] Hubei Key Laboratory of Mineral Resources Processing and Environment, School of Resources and Environmental Engineering, State Key Laboratory of Silicate Materials for Architectures, Wuhan University of Technology, Wuhan 430070, China

region in solar spectrum, stable physicochemical properties and better electron transport performance than those of TiO_2 [17–20]. Pristine WO_3 is a kind of yellow powder solid, in which oxygen atoms enclose the tungsten atoms to form a corner-sharing distorted octahedra. Oxygen atoms are at the corners of an octahedron and a tungsten atom occupies a center position of the octahedron. In fact, the structure of tungsten oxide is influenced by temperature: a triclinic structure exists from − 50 to 17 °C and then a monoclinic structure is stable from 17 to 330 °C. Above 330 °C and until 740 °C, an orthorhombic structure exists, and finally, above that temperature WO_3 becomes the tetragonal phase. The polymorphic property of WO_3 could form a phase junction to promote the photocatalytic activity for VOC degradation [21]. However, the unmodified WO_3 has a low light energy conversion efficiency as the reduction potential of the electrons in WO_3 is low, which accelerates the recombination rate of photo-generated electrons and holes. Some significant efforts are proposed to overcome this shortcoming such as doping [22], noble metal deposition [23] and coupling with other semiconductors [24]. Based on the published literature, despite abundant reported articles focusing on modifying WO_3-based photocatalysts, there is an absence of a review on the enhanced performance of tungsten-based photocatalysts for degradation of VOCs in the gas phase.

Here, we provide a short review to enable the reader to make connections among the morphology features, surface defects, electronic properties of the photocatalyst and stable photocatalytic activity toward varies VOCs. Therefore, this paper reviews modification techniques for overcoming the inherent WO_3 limitations and improving the photocatalytic activity of VOCs. Such techniques include controlling the morphology, introducing defects, coupling with heterojunction, doping ions and using co-catalyst. This paper also describes the challenges and research directions for the further exploration of VOCs degradation with tungsten-based photocatalysts in engineering applications.

2 Issues in photocatalytic oxidation of VOCs with tungsten oxide

Photocatalytic reactions for degradation of VOCs with semiconductor catalyst are a surface chemical oxidation process. This chemical reaction was focused on the critical process: the semiconductor realizes the band-gap energy requirement to generate chemical active species under the absorption of ultraviolet or visible radiation, then the primary oxidant species (hydroxyl radicals), which are formed by oxidizing adsorbed OH^- or adsorbed water for oxidation of VOCs [25]. This oxidation of VOCs include some processes such as adsorption of VOCs in gas phase onto the surface of semiconductors, separation of the electrons and holes and transferring to the surface of semiconductors, generation of reactive oxygen species (ROS) to facilitate chemical degradation, and the desorption of products or intermediates [26]. However, the photocatalysis oxidation of VOCs on surface of some semiconductors exist some inherent drawbacks such as the easy recombination of photogenerated electrons and holes on the surface of the semiconductor materials [27], which impeded the production of ROS.

In addition, compared with the photocatalytic degradation of wastewater in liquid phase, the solid semiconductor catalyst is difficult to evenly disperse in the VOCs pollutants, which restricts the full contact between the catalyst and pollutants. Although advanced and precision characterization and calculation methods are used to research the relationship between the catalyst and pollutants [28, 29], the reaction mechanism for VOCs degradation is still complex, which impedes further research to photocatalytic reactions. Furthermore, it is testified that the deactivation of photocatalysts is closely related to the reactive intermediates of VOCs, which is a main barrier that diminishes the value of practical applications for photocatalytic VOCs degradation [30]. Besides, the complex pollutant composition and rigorous reaction conditions lead to a challenge of confirming the surface oxidation mechanisms for VOC degradation.

As a promising photocatalyst, tungsten trioxide has many advantages, such as strong adsorption with gas phase pollutants, substantial utilization of the abundant solar spectrum, exceptional photochemical stability and resilience to reaction condition effects [31]. However, the low conduct band (CB) location of W-containing single oxide semiconductor has an inferior reductive potential, which restricts their capacity for reduction of oxygen and results in an accumulation of free electrons, then followed by an increased incidence to recombine with holes, which leads to a low conversion efficiency for light energy [32–34]. Therefore, WO_3 with modification is thought to be appropriate for VOCs decomposition.

3 Strategies for improving the VOCs photocatalytic oxidation performance with modified WO_3

3.1 Controlling the morphology structure of WO_3

In general, WO_3 semiconductors with smooth and porous surface areas are beneficial to improve their photocatalytic performance [35–37]. The methods of hydrothermal reactions and template-mediated synthesis were used by Sayama et al. [38] for preparing five WO_3 samples (WO_3 prepared from amorphous peroxo-tungstic acid-WO_3 (PA), and WO_3 powder was prepared by calcination-WO_3 (C), mesoporous WO_3, homemade WO_3 powder and commercial WO_3), acting as various photocatalysts to degradation of hexane. WO_3

(PA) showed a higher photocatalytic activity and more efficient absorption than those of other samples in visible light region because of its special morphology. The flat and smooth morphology of WO_3 (PA) with a relatively large particle were measured by an optical microscope. In contrast, in all the other investigated samples with large aggregates, very rough surface morphologies were observed. Those sample powders showed large light reflection because of Mie scattering, which showed low photocatalytic activity for hexane degradation [39]. However, the small roughness and large surface porosity of the WO_3 (PA) powder reduced light reflection, which would improve the light absorption and enhance the high activity for hexane degradation.

The various morphologies of tungsten trioxide nanosheets were also synthesized by Wicaksana et al. [40] to research the size and crystallinity of the nanocube structure, nanobundle structure and nanoparticle structure of WO_3 in Fig. 1, which can be achieved by adjusting the pH of aqueous solution and regulating the concentration of sulfate precursors. The WO_3 nanocubes exhibit greater conversion of ethylene than those of the nanobundles and nanoparticles due to the cuboid morphology with more "edged" nature, which reduce the recombination of photogenerated electron–hole. Xie et al. [41] reported that WO_3 in a sheet-like structure could increase the reduction potential of the conduction compared to the cuboid structure because the dominance of the exposed crystal facets blue-shifted the band-gap of the WO_3 in a sheet-like form, contributing to the enhanced photo activity of photocatalytic water oxidation and pollutants degradation.

3.2 Defect modification

Defects in tungsten oxide materials can exhibit strong adsorption capability towards VOCs [42–45]. Wang et al. [46] reported oxygen vacancies can act as active sites on the VOC degradation of WO_3. The results showed that oxygen vacancies from WO_{3-x} can capture oxygen atoms from the formaldehyde and H_2O, which boost the production of hydroxyl radicals and lead to the oxidization and degradation of formaldehyde and benzene. Lu et al. [47] reported that tungsten oxide nanowire bundles with high concentration of oxygen vacancies provided an efficient activity for ethanol dehydration. The oxygen vacancies

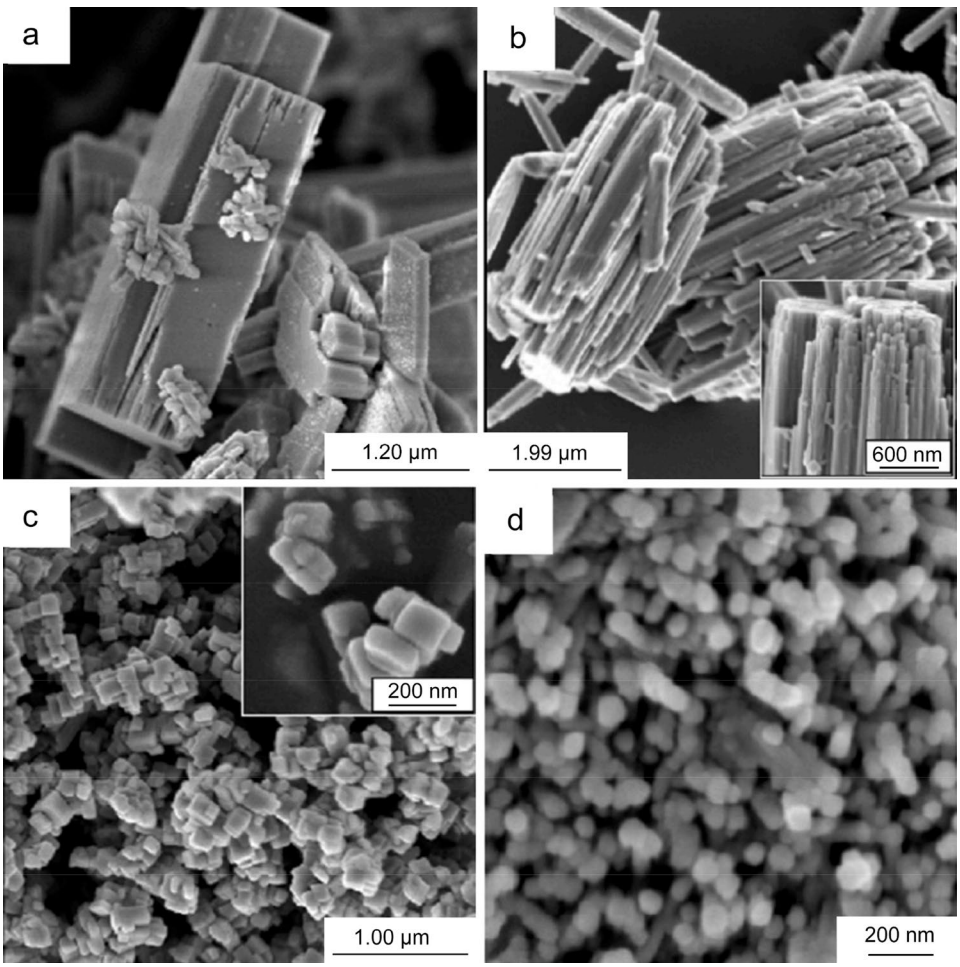

Fig. 1 SEM image for the different sharp distribution of WO_3 structure. **a** WO_3 morphology of slabs with columnar clusters; **b** WO_3 morphology of nanobundles; **c** WO_3 morphology of nanocubes; **d** WO_3 morphology of nanoparticles. Reproduced with permission from Ref. [40] Copyright 2014 MDPI

facilitate full utilization for solar energy and serve as active sites for the improvement of ethanol adsorption and degradation. Action mechanism and oxidation process of WO_{3-x} as photocatalyst were also illustrated in Fig. 2. Defect band (DB) can be formed to serve as an intermediate bridge to induce and transfer hot electrons and hot holes by the oxygen vacancy of WO_{3-x} materials, which can generate the plasmonic thermal effect under full-spectrum light irradiation in Fig. 2a, and then ethanol dehydrogenation and dehydration process would be informed. Finally aldehyde is generated, which was discussed in Fig. 2b.

Similar work was carried out by Bai et al. [48], who synthesized self-organized $W_{18}O_{49}$ nanowires with high oxygen vacancy concentrations via a facile one-pot method. Depending on the defect structure caused by oxygen vacancy, the $W_{18}O_{49}$ nanowires show unexpected selectivity in photocatalytic dehydration of isopropyl alcohol to propylene.

3.3 Heterojunction constructing

Doping hybrid WO_3 with other semiconductor to form a heterojunction is well-investigated to be an effective way for improving the separation efficiency of the photo-generated charges or extending the spectral response to full light region [49, 50].

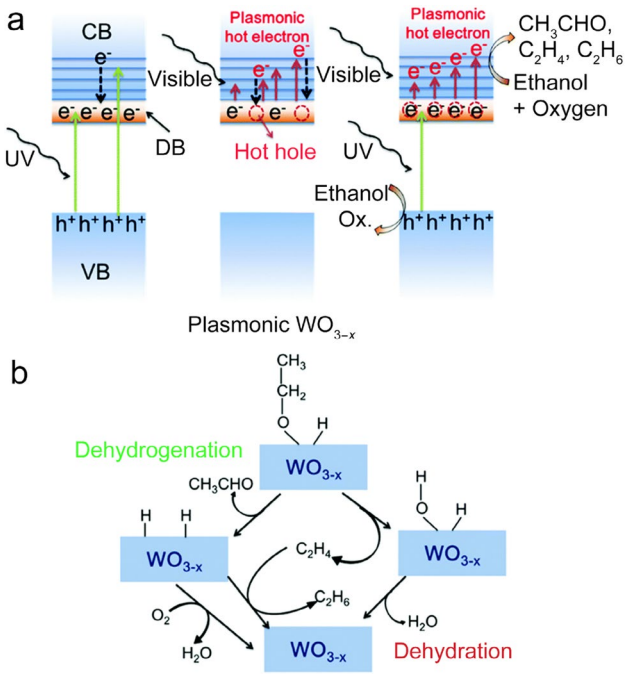

Fig. 2 **a** Photoelectron and hot electron generation in plasmonic WO_{3-x} under different light irradiation. **b** Dehydrogenation and dehydration of ethanol over WO_{3-x} as photocatalysts. Reproduced with permission from Ref. [47] Copyright 2019 Elsevier

3.3.1 WO_3/TiO_2 heterojunction

TiO_2 is a practical photocatalyst due to its strong oxidation power and low material cost. It has been reported that the formation of WO_3/TiO_2 heterojunction semiconductor can be used as an effective photocatalyst for degradation of VOCs [51, 52]. Zhang et al. [53] reported a hydrothermal method of the electrospun TiO_2 nanofibers to fabricate heterostructured TiO_2/WO_3 nanocomposites, which were loaded onto the inner walls of the photoreactor and fixed with nylon meshes to enhance the contact area between photocatalysts and toluene. The TiO_2/WO_3 nanocomposites showed a higher toluene degradation degree (85.3%) in flowing air than those of the TiO_2 nanofibers and the WO_3 nanoparticles. Single crystal structure of WO_3 nanorods that closely contacts with the TiO_2 nanofibers can reduce resistance of electrons transmission between the grain boundaries of TiO_2/WO_3 nanocomposites and accelerate the separation of the photo-generated carriers to improve the photocatalytic performance. To further research, the Z-scheme-type mechanism and heterojunction-type mechanism were compared to discuss the efficient photocatalytic decomposition of hexane in Fig. 3 [54]. According to the fluorescence spectra experiments, the heterojunction-type mechanism is more probable to expound the photocatalytic process of vaporous hexane degradation. The photogenerated electrons are stably transferred from the N-doped TiO_2 conduction band to that of WO_3, accelerating the generation of superoxide, while the hydroxyl radicals are formed by the hole reaction with water and hydroxyl ions, and the hazardous hexane molecules then are decomposed into some intermediate products, such as CO_2 and H_2O.

3.3.2 WO_3/carbon based heterojunction

Recently, graphitic carbon nitride is the widely used photocatalyst because of its high reduction ability, chemical stability and visible-light absorption [55]. Although the composite photocatalysts $WO_3/g\text{-}C_3N_4$ are applied in solar cells, splitting of water and carbon dioxide storage [56–58], their photocatalytic application in degradation of volatile organic pollutants are not common. $g\text{-}C_3N_4$ blended with WO_3 was successfully synthesized using a planetary mill by Jin et al. [59]. Compared with original samples, WO_3 nanosheets loaded with $g\text{-}C_3N_4$ particles exhibited a high activity for decomposition of acetaldehyde. The more positive valence band (VB) potential of WO_3 with high oxidation ability and more negative CB potential of $g\text{-}C_3N_4$ with superior reduction ability were utilized by the composite photocatalyst to accelerate

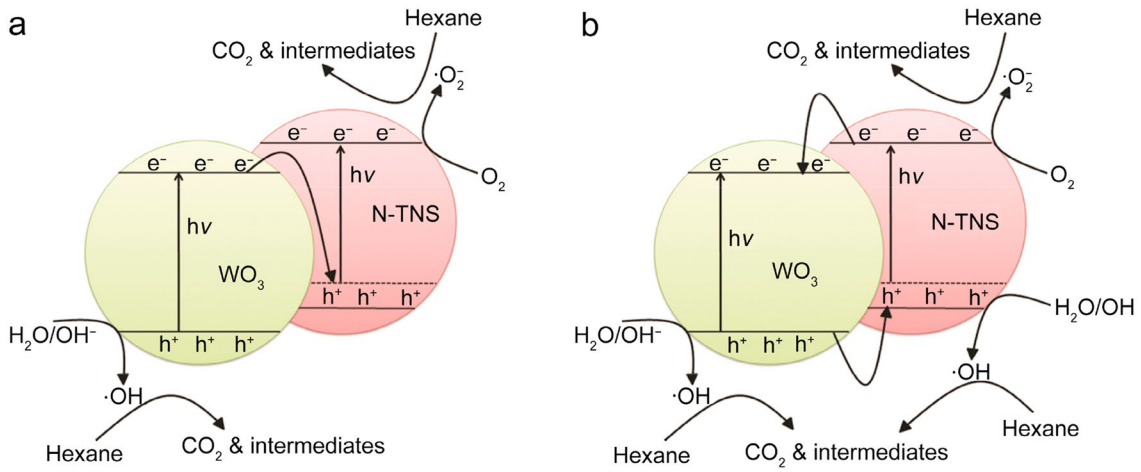

Fig. 3 **a** Z-scheme- and **b** heterojunction-type mechanisms involving N-doped TiO_2/WO_3 composite catalyst for the decomposition of hexane. Reproduced with permission from Ref. [54] Copyright 2016 Elsevier

electron separate and transfer from WO_3 to g-C_3N_4, which enhanced the complete oxidation of acetaldehyde. Similar research with photodegradation of acetaldehyde (HCHO) under visible-light irradiation was reported by Katsumata et al. [60]. Meanwhile, the enhanced visible-light-driven mechanism for g-C_3N_4/WO_3 composites were discussed. Some of the photoinduced electrons in carbon nitride surfaces are separated and transferred to the CB of WO_3, and partial photogenerated holes in WO_3 surfaces are transferred to the VB of g-C_3N_4. This cyclic process enhances the formation of free radicals such as superoxide and hydroxyl radicals.

In addition, ternary heterojunctions such as $CaFe_2O_4/WO_3$ [61] and $CuBi_2O_4/WO_3$ [62] were also reported for enhanced oxidation of VOCs.

3.4 Doped with WO_3

As a photocatalyst with a relatively wide band-gap, WO_3 is motivated by the near ultraviolet and blue regions of the solar spectrum. Doping WO_3 with different elements such as Mg [63], Cs [64], Zn [65], and Bi [66] to narrow the band-gap and increase the photocatalytic performance of WO_3 were reported. To enhance the absorption of visible light and effective transformation of photo-generated electron–holes, Fe ions were introduced, which can narrow the band-gap of WO_3 [67]. Sheng et al. [68] reported an interesting Fe-doped WO_3 catalytic material strongly adhered on a wood rabbit craft. This rabbit craft sample doped Fe (the content is 4.56%) showed a 98.21% degradation rate of formaldehyde in 6 h. The detailed photocatalytic reaction mechanism of HCHO was also proposed in Fig. 4: Fe^{3+} as a scavenger can not only trap the

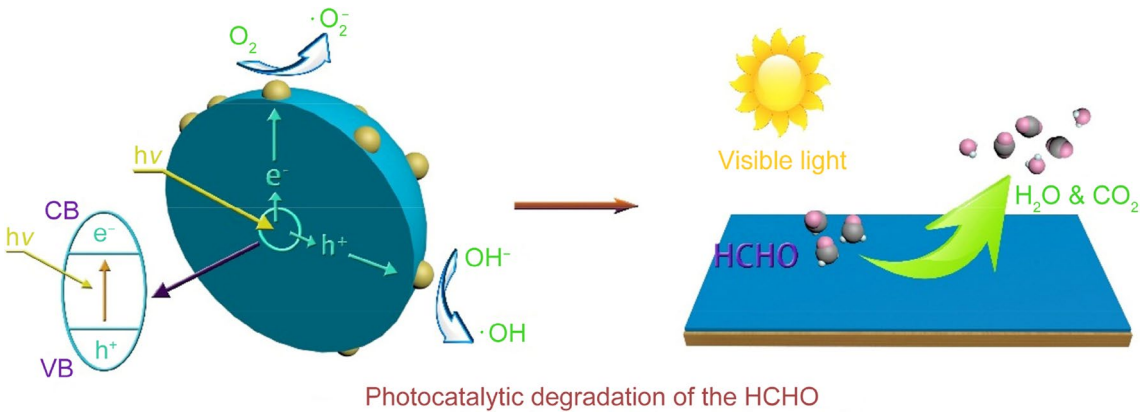

Fig. 4 Mechanism of photocatalytic degradation of HCHO by wood covered with Fe-doped WO_3. Reproduced with permission from Ref. [68] Copyright 2016 Elsevier

electrons and holes of WO_3 to prevent the recombination of excited charge carriers, but also participate in the oxidation reactions with hydroxyl ions and oxygen to form hydroxyl radicals and superoxide radicals, and then these energetic free radicals attack formaldehyde to form the final product such as CO_2 and H_2O. Irie et al. [69] also did the similar work through doped Cu(II) into the interior structure of WO_3, which exhibits 16 times higher photocatalytic ability for 2-propanol decomposition than that of N-doped TiO_2.

3.5 Cocatalyst loading

Loading a cocatalyst with tungsten oxide were extensively studied in utilization of solar energy to remove harmful organic pollutants in gaseous phase [70–75].

3.5.1 Noble metal co-catalyst

Noble metal (Pt, Ag and Pd) loaded onto WO_3 were confirmed to be a promising photocatalyst attributed to the surface plasmon resonance effect of noble metal nanoparticles, which can accelerate the effective transfer of free charges to the surface of WO_3 and facilitate the generation of active free radicals [76–78]. Zhao et al. [79] researched that loading appropriate Pt nanoparticles onto WO_3 can enhance photocatalytic activity for removal of acetaldehyde. Meanwhile, 0.5 wt% Pt-loaded WO_3 photocatalyst showed a complete decomposition of isopropyl alcohol, which was also reported by Abe et al. [80].

In addition, the photocatalytic properties of silver nanoparticles loaded on tungsten oxide nanocrystals in photocatalytic oxidation of cyclohexane were also researched by Xiao et al. [81]. A probable mechanism of Ag-WO_3 nanoparticles with high photocatalytic activity was showed in Fig. 5. The Ag nanoparticles loaded on WO_3 nanoparticles act as electronic traps to facilitate the electron-hole separation. Simultaneously, the surface plasmon resonance effect of Ag nanoparticles is attributed to the intense absorb ability of visible light, and then the electromagnetic fields near the surface of Ag nanoparticles is enhanced, which can facilitate the formation of main hydroxyl radicals and easily oxidize cyclohexane. A possible convention pathway for the photocatalytic oxidation of cyclohexane was proposed in Fig. 5b. Hydroxyl radicals (OH) and cyclohexyl peroxy radical (CyOO) are generated to trigger the radical oxidation process, which would selectively oxidize cyclohexane into cyclohexanol and cyclohexanone.

3.5.2 Loading other cocatalysts

Loading cocatalysts on tungsten oxide, such as carbon nanomaterial and base metal nanomaterial were reported to decomposition of VOCs under visible light irradiation

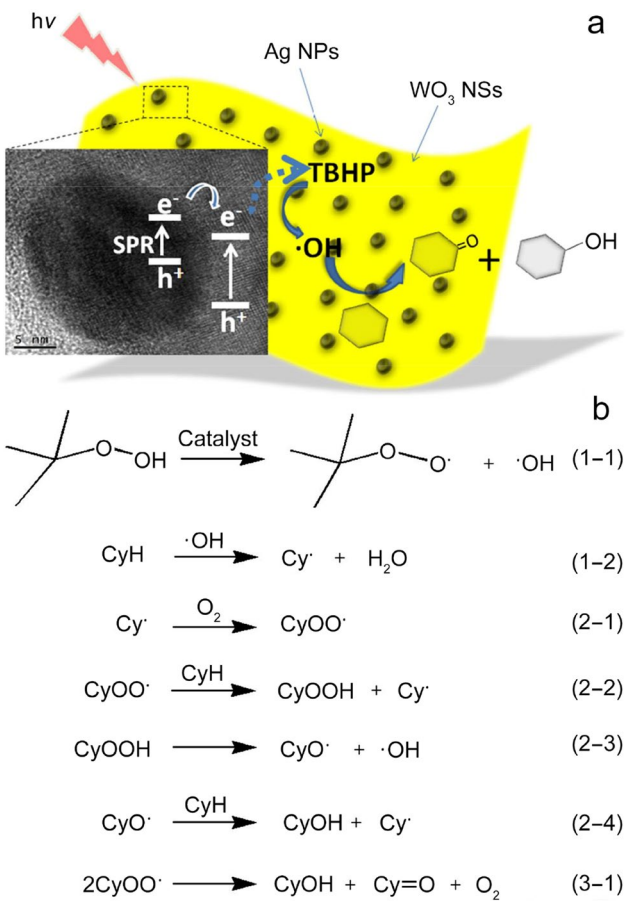

Fig. 5 Scheme of a the mechanism and b probable pathway for the photocatalytic oxidation of cyclohexane using Ag-loaded WO_3 composite as the catalyst. Reproduced with permission from Ref. [81] Copyright 2018 Elsevier

[82–84]. Kim et al. [85] prepared a carbon nanomaterial with a core–shell structure, which was loaded with WO_3 and applied for the degradation of acetaldehyde and toluene under visible light. Such superior activity of nanodiamond/WO_3 is attributed to the graphitic carbon shell on the diamond core, which can promote the charge separation and interfacial electron transfer. Recently, Fukumura et al. [86] synthesized a transparent thin layer photocatalyst, which was formed by a simple physical mixture of WO_3 nanoparticles and colloidal CeO_2. Further research revealed that CeO_2 might behave as a provider of reactive oxygen species in the thin layer photocatalyst system, which promote the degradation reaction of acetaldehyde.

A performance comparison of the modified WO_3-based photocatalysts, including the photocatalyst, photocatalytic efficiencies, VOC initial concentration et al., is presented in Table 1. It strongly suggests that modified WO_3-based photocatalysts are able to efficiently decompose varies of organic compounds. Furthermore, available data from Table 1 shows that coupling heterojunction and loading a noble metal may

Table 1 Comparison of WO_3-based photocatalysts for VOC degradation

Photocatalyst	Catalyst dose (mg)	Pollutant	VOC initial concentration (ppm)	Light source and Irradiation time	Photocatalytic efficiency (%)	References
Mesoporous WO_3	50	Acetic acid	250	300 W xenon lamp; 120 min	85[a]	[35]
Mesoporous WO_3	5	Ethanol	500	UV–vis (near NIR light irradiation); 180 min	90.5[b]	[37]
WO_3 with smooth and porous surface	150	Propane	22,700	Xenon lamp (400-500 nm); 600 min	99.8[a]	[38]
Mesoporous WO_3 with nanocube	60	Ethylene	508	Black light blue lamp; 30 min	28[b]	[40]
WO_3 with O vacancies	50	Formaldehyde	100	300 W Xe lamp; 90 min	97.6[a]	[46]
WO_3 with O vacancies	5	Ethanol	2000	300 W Xe lamp; 180 min	91[b]	[47]
WO_3/Bi_3O_4Cl heterojunction	100	Isopropanol	117	300 W Xe lamp; 120 min	100[a]	[50]
$WO_3/TiO_2/SnO_2$ heterojunction	100	1,2-dichlorobenzene	100	UV light (12 W); 240 min	95[a]	[51]
WO_3/TiO_2 heterojunction	25	Toluene	368	Fluorescent lamp; 480 min	85.3[a]	[53]
$WO_3/g\text{-}C_3N_4$ heterojunction	–	Acetaldehyde	1000	Light-emitting diode; 2880 min	100[a]	[59]
$WO_3/g\text{-}C_3N_4$ heterojunction	50	Acetaldehyde	250	Fluorescent light lamp; 2880 min	100[a]	[60]
Fe-doped WO_3	1000	N-pentane	31.5	Mercury lamp (125 w); 120 min	99.91[a]	[67]
Fe-doped WO_3	57.6	Formaldehyde	24	LED-light; 360 min	98.21[a]	[68]
Cu-doped WO_3	300	2-Propanol	300	Xe lamp; 2880 min	82.3[a]	[69]
WO_3/Co–Pt	10	Cyclohexane	100	300 W Hg lamp; 720 min	93[b]	[70]
WO_3/Co–Pt	50	Acetic acid	1100	300 W Xe lamp; 180 min	92.6[a]	[73]
WO_3/Co–Pt	100	Acetaldehyde	60	Xe lamp; 20 min	100[a]	[76]
WO_3/Co-Ag	200	Acetaldehyde	100	500 W Xe lamp; 60 min	90[a]	[77]
WO_3/Co-Pd	50	Acetaldehyde	5	Fluorescent-lamp; 240 min	100[a]	[78]
WO_3/Co-CuO	–	Acetaldehyde	9000	300 W Xe lamp; 360 min	100[a]	[84]
WO_3/Co- nanodiamond	100	Acetaldehyde	100	Halogen lamp; 90 min	92.1[b]	[85]
WO_3/CeO_2	130	Acetaldehyde	3500	UV lamp (300 W); 300 min	75.3[a]	[86]

[a]Mineralization efficiencies calculated based on the amount of CO_2 produced

[b]Conversion efficiencies calculated from the amount of VOC reduced

be effective methods to the degradation of different target VOCs. Although the performance of removing VOCs with modified tungsten-based catalyst were improved in many researches, there is still a problem to evaluate the photocatalytic oxidation performance on an objective basis and confirm the best photocatalytic material in uniform standards, as each relevant photocatalytic study on VOCs was carried out using different target VOCs and various experimental conditions. There is a long way between the laboratory research achievement and requirements for practical applications.

4 Conclusion and outlooks

This review proposed the issues of photocatalytic degradation of VOCs with tungsten oxide and summarized a series of strategies for improving the performance of WO_3-based catalyst in degradation of VOCs. It is indicated that all the enhancement of the photocatalytic efficiency for degradation of VOCs are concluded following four aspects: (1) broaden light absorption; (2) increase the active reactive sites on the surface of the modified WO_3-based photocatalyst, (3) extend the reaction surface area between the WO_3-based photocatalyst and VOCs; (4) boost the separation of the photogenerated carriers and inhibit the recombination of charge carriers. The relationship between the various strategies and their possible enhancement mechanisms include: (1) controlling the WO_3 morphology and doping suitable dopants, which can increase the light absorption; (2) forming WO_3 defect structure that can serve as active sites and enhance the adsorptivity with VOCs; (3) introducing a heterojunction with other semiconductor, which can promote the separation of the photogenerated carriers; (4) loading co-catalyst that can also facilitate the effective charge transfer due to the

surface plasmon resonance effect or good electrical conductivity of nanophase materials.

Although the performance of removing VOCs with modified tungsten-based catalyst were improved in many researches, there are still a lot of opportunities to enhance the photocatalytic efficiency of WO_3-based photocatalysts for removal of VOCs. Here, several research directions are proposed as reference for confirming the best photocatalytic material and proper practical applications.

(1) Although a series of strategies are developed for improving the performance of WO_3-based catalyst in degradation of VOCs, it is necessary to introduce synergistic effects with different strategies, which may lead to incredible photocatalytic performance than that of single strategies.
(2) The deep mechanism of WO_3-based photocatalysts for removal of VOCs is still vague. For instance, the charge-transfer dynamics and construction of heterojunctions mechanism still exist much controversy and lack of theoretical guidelines. Besides, advanced and precision characterization and calculation methods should be applied for VOC degradation, such as in situ Fourier transform infrared spectroscopy and density functional theory calculations.
(3) A further challenge should be focused on the development of efficient photocatalysts to solve practical problems. In addition, the efficient utilization of solar energy and lamplight should be highlighted in environmental purification. For example, photo-reactors can be designed for treatment of high concentration VOCs in chemical industries under solar energy, and the tungsten-based catalyst can be attached to the furniture to remove VOCs of indoor air under incandescent lamp. Therefore, there are still a lot of challenges and concerns to be addressed for providing prioritization solutions on VOCs degradation in the future.

Acknowledgements This work was financially supported by the National Natural Science Foundation of China (NSFC, Grant No. 51472194), the NSF of Hubei Province (Grant No. 2016CFA078) and the National Basic Research Program of China (973 Program, Grant No. 2013CB632402).

References

1. Cheng YH, Lin CC, Hsu SC. Comparison of conventional and green building materials in respect of VOC emissions and ozone impact on secondary carbonyl emissions. Build Environ. 2015;87:274.
2. Hoeben W, Beckers F, Pemen A, Heesch E, Kling WL. Oxidative degradation of toluene and limonene in air by pulsed corona technology. J Phys D Appl Phys. 2012;45:202.
3. Hubbard HF, Coleman BK, Sarwar G, Corsi RL. Effects of an ozone-generating air purifier on indoor secondary particles in three residential dwellings. Indoor Air. 2005;15(6):432.
4. Huang BB, Lei C, Wei CH, Zeng GM. Chlorinated volatile organic compounds (Cl-VOCs) in environment-sources, potential human health impacts, and current remediation technologies. Environ Int. 2014;71:118.
5. Lu Y, Liu J, Lu BN, Jiang AX, Wan CL. Study on the removal of indoor VOCs using biotechnology. J Hazard Mater. 2010;182(1):204.
6. Feng CY, Tang L, Deng YC, Wang JJ, Tang WW, Liu YN, Chen ZM, Yu JF, Wang JJ, Liang QH. Synthesis of branched WO_3@$W_{18}O_{49}$ homojunction with enhanced interfacial charge separation and full-spectrum photocatalytic performance. Chem Eng J. 2020;389:124474.
7. Li JJ, Yu EQ, Cai SC, Chen X, Chen J, Jia HP, Xu YJ. Noble metal free, CeO_2/$LaMnO_3$ hybrid achieving efficient photothermal catalytic decomposition of volatile organic compounds under IR light. Appl Catal B. 2019;240:141.
8. Vildozo D, Portela R, Ferronato C, Chovelon JM. Photocatalytic oxidation of 2-propanol/toluene binary mixtures at indoor air concentration levels. Appl Catal B. 2011;107(3):347.
9. Wang K, Wu XY, Zhang GK, Li J, Li Y. $Ba_5Ta_4O_{15}$ nanosheet/$AgVO_3$ nanoribbon heterojunctions with enhanced photocatalytic oxidation performance: hole dominated charge transfer path and plasmonic effect insight. Acs Sustain Chem Eng. 2018;6(5):6682.
10. Wang K, Li J, Zhang GK. Ag-bridged Z-scheme 2D/2D $Bi_5FeTi_3O_{15}$/g-C_3N_4 heterojunction for enhanced photocatalysis: mediator-induced interfacial charge transfer and mechanism insights. Acs Appl Mater Inter. 2019;11(31):27686.
11. Wang K, Li Y, Li J, Zhang GK. Boosting interfacial charge separation of $Ba_5Nb_4O_{15}$/g-C_3N_4 photocatalysts by 2D/2D nanojunction towards efficient visible-light driven H_2 generation. Appl Catal B. 2020;263:117730.
12. Mao L, Cai XY, Yang SQ, Han KL, Zhang JY. Black phosphorus-CdS-$La_2Ti_2O_7$ ternary composite: effective noble metal-free photocatalyst for full solar spectrum activated H_2 production. Appl Catal B. 2019;242:441.
13. Sun JC, Wang YY, Guo SQ, Wan BS, Dong LQ, Gu YD, Song C, Pan CF, Zhang QH, Gu L, Pan F, Zhang JY. Lateral 2D WSe_2 p-n homojunction formed by efficient charge-carrier-type modulation for high-performance optoelectronics. Adv Mater. 2020;32:1906499.
14. Yokosuka Y, Oki K, Nishikiori H, Tatsumi Y, Tanaka N, Fujii T. Photocatalytic degradation of trichloroethylene using N-doped TiO_2 prepared by a simple sol-gel process. Res Chem Intermediat. 2009;35(1):43.
15. Wang HP, Zhang L, Zhou YY, Qiao SM, Liu XC, Wang WZ. Photocatalytic CO_2 reduction over platinum modified hexagonal tungsten oxide: effects of platinum on forward and back reactions. Appl Catal B. 2020;263:118331.
16. Wei W, Yao YJ, Zhao Q, Xu ZL, Wang QF, Zhang ZT, Gao YF. Oxygen defect-induced localized surface plasmon resonance at the WO_{3-x} quantum dot/silver nanowire interface: SERS and photocatalysis. Nanoscale. 2019;11(12):5535.
17. Li WJ, Da PM, Zhang YY, Wang YC, Lin X, Gong XG, Zheng GF. WO_3 nanoflakes for enhanced photoelectrochemical conversion. ACS Nano. 2014;8(11):11770.
18. Lu Y, Li Y, Wang YY, Zhang JY. Two-photon induced NIR active core-shell structured WO_3/CdS for enhanced solar light photocatalytic performance. Appl Catal B. 2020;272:118979.
19. Dong PY, Hou GH, Xi XG, Shao R, Dong F. WO_3-based photocatalysts: morphology control, activity enhancement and multifunctional applications. Environ Sci-Nano. 2017;4(3):539.

20. Huang JW, Yue PF, Wang L, She HD, Wang QZ. A review on tungsten-trioxide-based photoanodes for water oxidation. Chin J Catal. 2019;40(10):1408.
21. Wijs GA, Boer PK, Groot RA. Anomalous behavior of the semiconducting gap in WO_3 from first-principles calculations. Phys Rev B. 1999;59(4):2684.
22. Bao K, Zhang SJ, Ni P, Zhang ZX, Zhang KL, Wang LB, Sun LX, Mao WT, Zhou QF, Qian YT. Convenient fabrication of carbon doped WO_{3-x} ultrathin nanosheets for photocatalytic aerobic oxidation of amines. Catal Today. 2020;340:311.
23. Shi HX, Yang SZ, Han C, Niu ZJ, Li HH, Huang XB, Ma JC. Fabrication of $Ag/Ag_3PO_4/WO_3$ ternary nanoparticles as superior photocatalyst for phenol degradation under visible light irradiation. Solid State Sci. 2019;96(4):105967.
24. Claudino CH, Kuznetsova M, Rodrigues BS, Chen CQ, Wang ZY, Sardela M, Souza JS. Facile one-pot microwave-assisted synthesis of tungsten-doped $BiVO_4/WO_3$ heterojunctions with enhanced photocatalytic activity. Mater Res Bull. 2020;125:110783.
25. Tseng TK, Lin YS, Chen YJ, Chu H. A review of photocatalysts prepared by sol-gel method for VOCs removal. Int J Mol Sci. 2010;11(6):2336.
26. Feng YC, Li L, Ge M, Guo CS, Wang JF, Liu L. Improved catalytic capability of mesoporous TiO_2 microspheres and photodecomposition of toluene. Acs Appl Mater Inter. 2010;2(11):3134.
27. Chen H, Nanayakkara CE, Grassian VH. Titanium dioxide photocatalysis in atmospheric chemistry. Chem Rev. 2012;112(11):5919.
28. Chen LC, Cui W, Li JY, Wang H, Dong XA, Chen P, Zhou Y, Dong F. The high selectivity for benzoic acid formation on $Ca_2Sb_2O_7$ enables efficient and stable toluene mineralization. Appl Catal B. 2020;271:118948.
29. Li KL, He Y, Chen P, Wang H, Sheng JP, Cui W, Leng G, Chu YH, Wang ZM, Dong F. Theoretical design and experimental investigation on highly selective Pd particles decorated C_3N_4 for safe photocatalytic NO purification. J Hazard Mater. 2020;392:122357.
30. Chen P, Cui W, Wang H, Dong XA, Li JY, Sun YJ, Zhou Y, Zhang YX, Dong F. The importance of intermediates ring-opening in preventing photocatalyst deactivation during toluene decomposition. Appl Catal B. 2020;272:118977.
31. Mamaghani AH, Haghighat F, Lee CS. Photocatalytic oxidation technology for indoor environment air purification: the state-of-the-art. Appl Catal B. 2017;203:247.
32. Zou WX, Gao B, Ok YS, Dong L. Integrated adsorption and photocatalytic degradation of volatile organic compounds (VOCs) using carbon-based nanocomposites: a critical review. Chemosphere. 2019;218:845.
33. Zhu T, Chong MN, Chan ES. Nanostructured tungsten trioxide thin films synthesized for photoelectrocatalytic water oxidation: a review. Chemsuschem. 2014;7(11):2974.
34. Tsang CH, Li K, Zeng YX, Zhao W, Zhang T, Zhan YJ, Xie RJ, Leung DY, Huang HB. Titanium oxide based photocatalytic materials development and their role of in the air pollutants degradation: overview and forecast. EnvironInt. 2019;125:200.
35. Usami Y, Hongo T, Yamazaki A. Phosphate constituent effects on the structure and photocatalytic properties of mesoporous tungsten oxides. Micropor Mesopor Mat. 2012;158:13.
36. Hagstrom AL, Weon S, Choi WY, Kim JH. Triplet-triplet annihilation upconversion in broadly absorbing layered film systems for sub-bandgap photocatalysis. Acs Appl Mater Int. 2019;11(14):13304.
37. Li J, Chen GY, Yan JH, Huang BB, Cheng HF, Lou ZZ, Li BJ. Solar-driven plasmonic tungsten oxides as catalyst enhancing ethanol dehydration for highly selective ethylene production. Appl Catal B. 2020;264:118517.
38. Sayama K, Hayashi H, Arai T, Yanagida M, Gunji T, Sugihara H. Highly active WO_3 semiconductor photocatalyst prepared from amorphous peroxo-tungstic acid for the degradation of various organic compounds. Appl Catal B. 2010;94(1–2):150.
39. Herklotz A, Rus SF, Sohn C, Santosh KC, Cooper VR, Guo EJ, Ward TZ. Optical response of $BiFeO_3$ films subjected to uniaxial strain. Phys Rev Mater. 2019;3(9):094410.
40. Wicaksana Y, Liu S, Scott J, Amal R. Tungsten trioxide as a visible light photocatalyst for volatile organic carbon removal. Molecules. 2014;19(11):17747.
41. Xie YP, Liu G, Yin LC, Cheng HM. Crystal facet-dependent photocatalytic oxidation and reduction reactivity of monoclinic WO_3 for solar energy conversion. J Mater Chem. 2012;22(14):6746.
42. Lou ZZ, Xue C. In situ growth of WO_{3-x} nanowires on g-C_3N_4 nanosheets: 1D/2D heterostructures with enhanced photocatalytic activity. CrystEngComm. 2016;18(43):8406.
43. Zhao Y, Balasubramanyam S, Sinha R, Lavrijsen R, Verheijen MA, Bol AA, Bieberle-Hütter A. Physical and chemical defects in WO_3 thin films and their impact on photoelectrochemical water splitting. ACS Appl Energy Mater. 2018;1(11):5887.
44. Chen PQ, Qin ML, Liu Y, Jia R, Cao ZQ, Wan Q, Qu XH. Superior optical properties of Fe^{3+}-$W_{18}O_{49}$ nanoparticles prepared by solution combustion synthesis. N J Chem. 2015;39(2):1121.
45. Lou ZZ, Gu Q, Xu L, Liao YS, Xue C. Surfactant-free synthesis of plasmonic tungsten oxide nanowires with visible-light-enhanced hydrogen generation from ammonia borane. Chemistry. 2015;10(6):1291.
46. Wang LY, Xu XX, Wu SJ, Cao F. Nonstoichiometric tungsten oxide residing in a 3D nitrogen doped carbon matrix, a composite photocatalyst for oxygen vacancy. Catal Sci Technol. 2018;8(5):1366.
47. Lu CH, Li J, Chen GY, Li BJ, Lou ZZ. Self-Z-scheme plasmonic tungsten oxide nanowires for boosting ethanol dehydrogenation under UV-visible light irradiation. Nanoscale. 2019;11(27):12774.
48. Bai H, Su N, Li WT, Zhang X, Yan Y, Li P, Ouyang SX, Ye JH, Xi GC. $W_{18}O_{49}$ nanowire networks for catalyzed dehydration of isopropyl alcohol to propylene under visible light. J Mater Chem A. 2013;1(20):6125.
49. Lee J, Jo WK. Three-dimensional TiO_2 structures incorporated with tungsten oxide for treatment of toxic aromatic volatile compounds. Catalysts. 2017;7(12):97.
50. Chakraborty AK, Kebede MA. Preparation and characterization of WO_3/Bi_3O_4Cl nanocomposite and its photocatalytic behavior under visible light irradiation. React Kinet Mech Cat. 2012;106(1):83.
51. Nadarajan R, Wan Abu Bakar WA, Ali R, Ismail R. Effect of structural defects towards the performance of $TiO_2/SnO_2/WO_3$ photocatalyst in the degradation of 1,2-dichlorobenzene. J Taiwan Inst Chem E. 2016;64:106.
52. Nadarajan R, Wan A, Ali R, Ismail R. Photocatalytic degradation of 1,2-dichlorobenzene using immobilized $TiO_2/SnO_2/WO_3$ photocatalyst under visible light: application of response surface methodology. Arab J Chem. 2018;11(1):34.
53. Zhang L, Qin MK, Yu W, Zhang QH, Xie HY, Sun ZG, Shao Q, Guo XK, Hao LH, Zheng YJ, Guo ZH. Heterostructured TiO_2/WO_3 nanocomposites for photocatalytic degradation of toluene under visible light. J Electrochem Soc. 2017;164(14):H1086.
54. Lee JY, Jo WK. Heterojunction-based two-dimensional N-doped TiO_2/WO_3 composite architectures for photocatalytic treatment of hazardous organic vapor. J Hazard Mater. 2016;314:22.
55. Groenewolt M, Antonietti M. Synthesis of g-C_3N_4 nanoparticles in mesoporous silica host matrices. Adv Mater. 2005;17(14):1789.
56. Li YG, Wei XL, Yan XY, Cai JT, Zhou AN, Yang MR, Liu KQ. Construction of inorganic-organic 2D/2D WO_3/g-C_3N_4 nanosheet arrays toward efficient photoelectrochemical splitting of natural seawater. Phys Chem Chem Phys. 2016;18(15):10255.
57. Han X, Xu DY, An L, Hou CY, Li YG, Zhang QH, Wang HZ. WO_3/g-C_3N_4 two-dimensional composites for visible-light

driven photocatalytic hydrogen production. Int J Hydrogen Energy. 2018;43(10):4845.
58. Huang SL, Long YJ, Ruan SC, Zeng YJ. Enhanced photocatalytic CO_2 reduction in defect-engineered Z-scheme WO_{3-x}/g-C_3N_4 heterostructures. ACS Omega. 2019;4(13):15593.
59. Jin ZY, Murakami N, Tsubota T, Ohno T. Complete oxidation of acetaldehyde over a composite photocatalyst of graphitic carbon nitride and tungsten(VI) oxide under visible-light irradiation. Appl Catal B. Environ. 2014;150–151:479.
60. Katsumata KI, Motoyoshi R, Matsushita N, Okada K. Preparation of graphitic carbon nitride (g-C_3N_4)/WO_3 composites and enhanced visible-light-driven photodegradation of acetaldehyde gas. J Hazard Mater. 2013;260:475.
61. Liu ZF, Zhao ZG, Miyauchi M. Efficient visible light active $CaFe_2O_4$/WO_3 based composite photocatalysts: effect of interfacial modification. J Phys Chem C. 2009;113(39):17132.
62. Arai T, Yanagida M, Konishi Y, Iwasaki Y, Sugihara H, Sayama K. Efficient complete oxidation of acetaldehyde into CO_2 over $CuBi_2O_4$/WO_3 composite photocatalyst under visible and UV light irradiation. J Phys Chem C. 2007;111(21):7574.
63. Hwang DW, Kim J, Park TJ, Lee JS. Mg-doped WO_3 as a novel photocatalyst for visible light-induced water splitting. Catal Lett. 2002;80(1):53.
64. Li Y, Wu XY, Li J, Wang K, Zhang GK. Z-scheme g-C_3N_4@ CsxWO$_3$ heterostructure as smart window coating for UV isolating, Vis penetrating, NIR shielding and full spectrum photocatalytic decomposing VOCs. Appl Catal B. 2018;229:218.
65. Cheng XF, Leng WH, Liu DP, Zhang JQ, Cao CN. Enhanced photoelectrocatalytic performance of Zn-doped WO_3 photocatalysts for nitrite ions degradation under visible light. Chemosphere. 2007;68(10):1976.
66. Kako T, Meng XG, Ye JH. Solid-base loaded WO_3 photocatalyst for decomposition of harmful organics under visible light irradiation. Appl Mater. 2015;3(10):104411.
67. Torabi MM, Nasiri M, Abedini E, Sharifnia S. Enhanced gas-phase photocatalytic oxidation of n-pentane using high visible-light-driven Fe-doped WO_3 nanostructures. J Environ Chem Eng. 2018;6(5):6741.
68. Sheng CM, Wang C, Wang HW, Jin C, Sun QF, Li S. Self-photodegradation of formaldehyde under visible-light by solid wood modified via nanostructured Fe-doped WO_3 accompanied with superior dimensional stability. J Hazard Mater. 2017;328:127.
69. Irie H, Miura S, Kamiya K, Hashimoto K. Efficient visible light-sensitive photocatalysts: grafting Cu(II) ions onto TiO_2 and WO_3 photocatalysts. Chem Phys Lett. 2008;457(1–3):202.
70. Shiraishi Y, Sugano Y, Ichikawa S, Hirai T. Visible light-induced partial oxidation of cyclohexane on WO_3 loaded with Pt nanoparticles. Catal Sci Technol. 2012;2(2):4.
71. Sakai Y, Shimanaka A, Shioi M, Kato S, Satokawa S, Kojima T, Yamasaki A. Fabrication of high-sensitivity palladium loaded tungsten trioxide photocatalyst by photodeposite method. Catal Today. 2015;241:2.
72. Higashimoto S, Katsuura K, Yamamoto M, Takahashi M. Photocatalytic activity for decomposition of volatile organic compound on Pt-WO_3 enhanced by simple physical mixing with TiO_2. Catal Commun. 2020;133:105831.
73. Sadakane M, Sasaki K, Kunioku H, Ohtani B, Ueda W, Abe R. Preparation of nano-structured crystalline tungsten(vi) oxide and enhanced photocatalytic activity for decomposition of organic compounds under visible light irradiation. Chem Commun. 2008;48:6552.
74. Jansson I, Yoshiiri K, Hori H, García FJ, Rojas S, Sánchez B, Ohtani B, Suárez S. Visible light responsive Zeolite/WO_3–Pt hybrid photocatalysts for degradation of pollutants in air. Appl Catal A Gen. 2016;521:208.
75. Ueyama K, Hatta T, Okemoto A, Taniya K, Ichihashi Y, Nishiyama S. Cyclohexane photooxidation under visible light irradiation by WO_3–TiO_2 mixed catalysts. Res Chem Intermediat. 2018;44(1):629.
76. Oka N, Murata A, Nakamura S, Jia J, Iwabuchi Y, Kotsubo H, Shigesato Y. Visible-light active thin-film WO_3 photocatalyst with controlled high-rate deposition by low-damage reactive-gas-flow sputtering. Apl Mater. 2015;3(10):104407.
77. Sun S, Wang WZ, Zeng SZ, Shang M, Zhang L. Preparation of ordered mesoporous Ag/WO_3 and its highly efficient degradation of acetaldehyde under visible-light irradiation. J Hazard Mater. 2010;178(1–3):427.
78. Arai T, Horiguchi M, Yanagida M, Gunji T, Sugihara H, Sayama K. Complete oxidation of acetaldehyde and toluene over a Pd/WO_3 photocatalyst under fluorescent- or visible-light irradiation. Chem Commun. 2008;43:5565.
79. Zhao ZG, Miyauchi M. Nanoporous-walled tungsten oxide nanotubes as highly active visible-light-driven photocatalysts. Angew Chem Int Edit. 2008;47(37):7051.
80. Abe R, Takami H, Murakami N, Ohtani B. Pristine simple oxides as visible light driven photocatalysts: highly efficient decomposition of organic compounds over platinum-loaded tungsten oxide. J Am Chem Soc. 2008;130(25):7780.
81. Xiao Y, Liu J, Mai J, Pan C, Cai X, Fang Y. High-performance silver nanoparticles coupled with monolayer hydrated tungsten oxide nanosheets: the structural effects in photocatalytic oxidation of cyclohexane. J Colloid Interface Sci. 2018;516:172.
82. Arai T, Horiguchi M, Yanagida M, Gunji T, Sugihara H, Sayama K. Reaction mechanism and activity of WO_3-catalyzed photodegradation of organic substances promoted by a CuO cocatalyst. J Phys Chem C. 2009;113(16):6602.
83. Kim H, Weon S, Kang H, Hagstrom AL, Kwon OS, Lee Y, Choi W, Kim JH. Plasmon-enhanced sub-bandgap photocatalysis via triplet-triplet annihilation upconversion for volatile organic compound degradation. Environ Sci Technol. 2016;50(20):11184.
84. Arai T, Yanagida M, Konishi Y, Iwasaki Y, Sugihara H, Sayama K. Promotion effect of CuO co-catalyst on WO_3-catalyzed photodegradation of organic substances. Catal Commun. 2008;9(6):1254.
85. Kim HI, Kim HN, Weon S, Moon GH, Kim JH, Choi W. Robust co-catalytic performance of nanodiamonds loaded on WO_3 for the decomposition of volatile organic compounds under visible light. Acs Catal. 2016;6(12):8350.
86. Fukumura T, Sambandan E, Yamashita H. Synthesis and VOC degradation ability of a CeO_2/WO_3 thin-layer visible-light photocatalyst. Mater Res Bull. 2017;94:493.

Dr. Gao-Ke Zhang is a professor of school of Resources and Environmental Engineering in Wuhan University of Technology (WUT). He received his Ph.D. degree from the school of Materials Science and Engineering, WUT, in 2004. From 2005 to 2006, he was an adjunct professor at Materials Research Institute, Pennsylvania State University, USA. He was awarded the Ministry of Education New Century Talent Support Program in 2005. He has published over 180 peer reviewed journals (*J. Am. Chem. Soc, Angew. Chem. Int. Ed, Environ. Sci. Technol, Appl. Catal. B:Environ., J. Mater: Chem.A, Acs. Appl. Mater. Inter,* ect.) and authorized over 20 invention patents. His research interests focus on clay-based materials, adsorption materials and novel photocatalysts for environmental applications.